Vol 14 No 2, February 2005
1009-1963/2005/14(02)/0311-06

Chinese Physics

© 2005 Chin. Phys. Soc.
and IOP Publishing Ltd

Local structural distortion and magnetotransport properties of $Nd_{0.5}Pb_{0.5-x}Sr_x$ (Mn, Fe)O_3*

Kou Zhi-Qi(寇志起)†, Di Nai-Li(邸乃力), Lu Yi(鲁 毅),
Ma Xiao(马 骁), Li Qing-An(李庆安), and Cheng Zhao-Hua(成昭华)

State Key Laboratory of Magnetism, Institute of Physics, Chinese Academic of Sciences, Beijing 100080, *China*

(Received 9 July 2004; revised manuscript received 27 September 2004)

Structural and magnetotransport properties of Fe-doped $Nd_{0.5}Pb_{0.5-x}Sr_xMnO_3$ are investigated by means of x-ray diffraction (XRD), Mössbauer spectroscopy and transport measurements. Both XRD patterns and Mössbauer spectra indicate that structural distortion decreases with Sr doping. Furthermore, it is found that Sr doping results in decrease of the resistivity at room temperature and increase of magnetoresistance. In samples, the same ratio of Mn^{3+} to Mn^{4+} is kept. So we would rather attribute these changes to the local structural distortion than the double exchange (DE) interaction. The local structural distortion of the Mn(Fe)O_6 octahedron which results from the Jahn–Teller effect, can localize the conduction electrons. In this regard, we provide another evidence to prove that this Jahn–Teller distortion is an important factor that affects the transport property above T_c besides the DE coupling.

Keywords: Mössbauer spectroscopy, Jahn–Teller distortion, colossal magnetoresistance
PACC: 0785, 7530V, 6110M

1. Introduction

Recently, colossal magnetoresistance (CMR) in hole-doped manganese oxides with a perovskite-type structure has been investigated extensively due to its diversified physical phenomena and potential applications.[1−3] It has been recognized that CMR in $Ln_{1-x}A_xMnO_3$ (Ln and A being rare-earth and alkaline-earth elements, respectively) involves the lattice effect due to a strong Jahn–Teller electron-phonon coupling in addition to the double exchange (DE) mechanism.[4−7] Local structural distortion of the MnO_6 octahedra plays an important role in determining the magnetotransport of doped holes and the complex magnetic and structural behaviour. A lattice distortion or a tilt of MnO_6 octahedra is related to the average ionic radius of Ln and A cations. Some studies recently indicated that the properties of $Ln_{1-x}A_xMnO_3$ varied systematically with the ionic radius of the A-site cation.[8−10] Pure $NdMnO_3$ has an orthorhombically distorted perovskite structure. However, the distortion has almost totally disappeared in this structure so that $Nd_{0.5}Pb_{0.5}MnO_3$ may be considered to be cubic.[11] Pb doping changes the symmetry of lattice structure. Although the substitution of divalent A atoms in such manganites has long been known to induce ferromagnetism and anomalous transport properties, the nature of the charge-carrier localization mechanism in the paramagnetic phase is still an unsolved important issue in the researches of these materials.[12]

The purpose of this paper is threefold. Firstly, in our previous paper,[13] we have studied the local Jahn–Teller distortion of Fe-doped $La_{1-x}Ca_xMnO_3$. In this paper, we change the crystal-electric field (CEF) only by changing the radius and property of divalent alkaline-earth elements in order to exclude the effect of the DE interaction. So we fix the concentration of Nd^{3+}ion. In this way, we also fix the ratio of Mn^{3+} to Mn^{4+} and ensure the same DE interaction. Secondly, we explore the change of structure in ceramic $Nd_{0.5}Pb_{0.5-x}Sr_xMn_{0.96}Fe_{0.04}O_3$ samples by x-ray diffraction (XRD) and Mössbauer spectroscopy. Because of the same radii of Mn^{3+} and Fe^{3+} ions (0.0645nm) in six-fold octahedral coordination,[14] the substitution of Fe^{3+} for Mn^{3+} does not change the tol-

*Project supported by the State Key Project of Fundamental Research of China (Grand No 2001CB610605) and the National Natural Science Foundation of China (Grand No 10274104).

†E-mail: kouzq@aphy.iphy.ac.cn

erance factor. The presence of a little Fe^{3+} ion also does not alter the distribution of surrounding electrons significantly. Although Fe^{3+} ion is not a Jahn–Teller ion, we can approximately assume that the CEF for FeO_6 and MnO_6 octahedra are similar. The quadruple splitting of Fe^{3+} is very sensitive to the distribution of surrounding electrons. So we can use it to detect the change of symmetry of the nearest-neighbour O^{2-} ions as a micro-probe. Thirdly, the Jahn–Teller effect can localize the conduction electrons. Transport measurements can demonstrate this kind of relationship.

2. Experimental procedures

Polycrystalline samples with nominal compositions of $Nd_{0.5}Pb_{0.5-x}Sr_xMn_{0.96}Fe_{0.04}O_3$ ($0.0 \leq x \leq 0.5$) were prepared by standard solid-state reaction. Stoichiometric proportions of Nd_2O_3, $SrCO_3$, $MnCO_3$, Fe_2O_3 and PbO powders with 99.99% purity were well mixed and preheated in air at 1073K for 12h. The powders were ground, pelletized and sintered at 1453K for 24h in mixed gases (70% Ar and 30% O_2) with several intermediary grindings, in order to prevent formation of impurity phases. The structure and phase purity of the prepared samples were checked by a Rigaku x-ray diffractometer with a rotating anode and Cu $K\alpha$ radiation. Temperature dependence of electrical resistivity of the samples was measured by a standard four-probe method.

^{57}Fe Mössbauer spectra were recorded by a Wissel system II constant acceleration Mössbauer spectrometer with a ^{57}Co(Rh) source at room temperature. The velocity was calibrated using an α-Fe foil. The values of isomer shift given here are relative to α-Fe at room temperature.

3. Results and discussion

XRD patterns prove that all samples of $Nd_{0.5}Pb_{0.5-x}Sr_xMn_{0.96}Fe_{0.04}O_3$ ($0.0 \leq x \leq 0.5$) are single-phase with an orthorhombically distorted perovskite structure (*Pbnm* space group). Rietveld profile refinement was carried out using the Hunter and Howard package to determine lattice constants and atomic positions.[15] Figure 1 shows the observed and fitted XRD patterns of $Nd_{0.5}Pb_{0.5-x}Sr_xMn_{0.96}Fe_{0.04}O_3$ (x=0.0, 0.3 and 0.5) compounds. The lattice parameters are listed in Table 1. The unit cell volume V contracts from 0.23238nm^3 to 0.22634nm^3 as x increases from 0.0 to 0.5. This is consistent with the ionic radius change of Pb^{2+} (0.120nm) to Sr^{2+} (0.112nm). In our study, the bond angle of Mn–O_2–Mn increases and that of Mn–O_1–Mn decreases with Sr doping. And the bond length Mn–O_1 decreases with increasing Sr concentration. According to the change of the bond angles and bond length, one can find that local structure distortion of Mn(Fe)O_6 octahedra decreases with increasing Sr concentration.

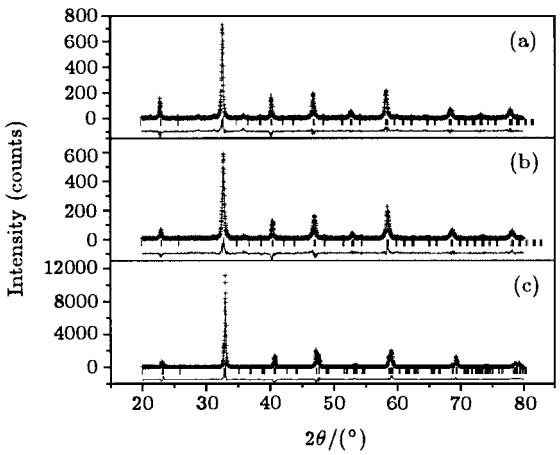


Fig.1. XRD patterns of $Nd_{0.5}Pb_{0.5-x}Sr_xMn_{0.96}Fe_{0.04}O_3$ (x=0.0 (a), 0.3 (b) and 0.5 (c)). The observed data and fitted pattern are indicated by cross and solid line, respectively. The lowest curves are the difference between observed and calculated patterns. The vertical bars indicated the expected reflection peak's position.

^{57}Fe Mössbauer spectra clearly indicate the presence of quadrupole splitting. For example, the Mössbauer spectra of $Nd_{0.5}Pb_{0.5-x}Sr_xMn_{0.96}Fe_{0.04}O_3$ (x=0.0, 0.3 and 0.5) at room temperature, illustrated in Fig.2, all can be best fitted with one doublet. For sample x=0.3, the doublet has a centre shift δ=0.319±0.012mm/s, and a quadrupole splitting Δ=0.358±0.020mm/s. This centre shift is a typical one of high-spin Fe^{3+} with octahedral coordination. One of the hyperfine parameters, the quadrupole splitting (Δ), is very sensitive to the change of the CEF which results from the Jahn–Teller distortion of Mn^{3+} around the resonant nuclei, and the smaller concentration of Fe (4 at %) does not alter the electronic and magnetic properties significantly. So its appearance proved the local distortion of the Mn(Fe)O_6 octahedron.

Table 1. Structure parameters of $Nd_{0.5}Pb_{0.5-x}Sr_xMn_{0.96}Fe_{0.04}O_3$ deduced from the Rietveld refinement of powder XRD data.

x	0.0	0.2	0.3	0.4	0.5
a/0.1nm	5.4903	5.4761	5.4747	5.4720	5.4666
b/0.1nm	5.4759	5.4632	5.4721	5.4295	5.4250
c/0.1nm	7.7296	7.7141	7.7187	7.6455	7.6322
$V/(0.1\text{nm})^3$	232.38	230.78	231.23	227.15	226.34
R_p/%	24.052	27.651	26.426	24.893	19.074
R_{wp}/%	33.435	36.081	35.792	34.246	25.347
χ^2	1.940	2.009	2.093	1.979	9.806
Mn-O_1-Mn	155.71	155.17	154.81	154.15	154.53
Mn-O_2-Mn	156.81	157.64	157.75	159.08	160.29
Mn-O_1	1.97664	1.97472	1.97727	1.96108	1.95615
Mn-O_2	1.95422	1.91410	2.00751	1.95413	1.95424
Mn-O_2	2.00371	2.02830	1.93690	1.96528	1.95422
$\langle$Mn-$O_2\rangle$	1.9789	1.9712	1.9722	1.9597	1.95423
Mn-$O_1/\langle$Mn-$O_2\rangle$	0.9988	1.0018	1.0025	1.0007	1.0009

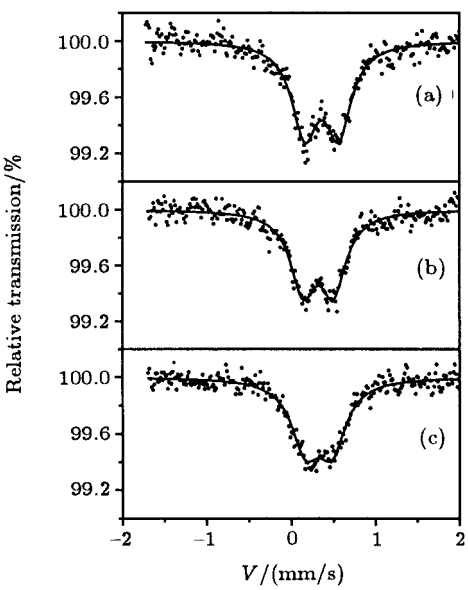


Fig.2. ^{57}Fe Mössbauer spectra of $Nd_{0.5}$ $Pb_{0.5-x}$ Sr_x $Mn_{0.96}$ $Fe_{0.04}O_3$ (x=0.0 (a), 0.3 (b), and 0.5 (c)) at room temperature.

In the case of ^{57}Fe Mössbauer effect, the quadrupole splitting, Δ, can be expressed as[16]

$$\Delta = \frac{eQV_{zz}}{2}\left(1+\frac{\eta^2}{3}\right)^{1/2}, \qquad (1)$$

where Q is the electric quadrupole moment of the ^{57}Fe nucleus, η is the asymmetry parameter. V_{zz} is the principal component of the electric field gradient (EFG) at the nucleus, which consists of contributions from valence electrons of both the Fe ion, V_{zz} (Fe), and the surrounding ions, V_{zz} (latt),

$$V_{zz}(\text{Fe}) = \sum_S P_S V_{zz}(s), \qquad (2)$$

$$V_{zz}(\text{latt}) = \sum_i \frac{q_i(3\cos^2\theta_i - 1)}{R_i^3} = \sqrt{\frac{5}{\pi}}A_{20}, \qquad (3)$$

where P_S is the probability of the valence electrons in different orbitals. $A_{20} = \sqrt{\frac{\pi}{5}}\sum_i \frac{q_i(3\cos^2\theta_i - 1)}{R_i^3}$ is the second-order CEF coefficient, and it is zero for cubic or perfectly octahedral symmetry. q_i is the electric charge of the ith surrounding ions. And R_i is the radial distance of the ith surrounding ions from the central ion, and θ_i is its polar angle in spherical coordinates. Thus, the contribution from the valence electrons of the Fe cations to the EFG at the nucleus depends on their configuration, i.e. the valence-state and spin-state. For high-spin Fe^{3+}, the half-filled shell is spherically symmetric regardless of the distribution of surrounding ions. Valence electrons of Fe ion have no contribution to EFG So we have

$$V_{zz}(\text{tot}) = V_{zz}(\text{latt}). \qquad (4)$$

The local structural distortion of Mn(Fe)O_6 octahedra results from the Jahn–Teller effect of Mn^{3+} ion, which removes the degeneracy of the e_g and t_{2g} orbitals. The energy splitting of the upper-level orbital is the main one. Since the Jahn–Teller distortion strongly influences the electron hopping process between the upper-level orbitals of Mn^{3+} and Mn^{4+} ions, and consequently determines the ferromagnetic and electrical behaviours, we only need to consider the upper-level splitting of e_g orbital. The energy separation of e_g orbital, E_{JT}, can be described as[17]

$$E_{JT} = 4D_s + 5D_t, \qquad (5)$$

$$D_s = \frac{e}{14}\sqrt{\frac{5}{\pi}}A_{20} < r^2 >_{3d}, \quad (6)$$

$$D_t = \frac{e}{14\sqrt{\pi}}T < r^4 >_{3d}, \quad (7)$$

where $T = A_{40}(\mathrm{oct}') - A_{40}(\mathrm{oct})$ is the difference between the fourth-order CEF coefficient of a distorted MnO_6 octahedron, $A_{40}(\mathrm{oct}')$ and that for perfect octahedral symmetry, $A_{40}(\mathrm{oct})$, where $A_{40} = \frac{\sqrt{\pi}}{4}\sum_i \frac{q_i}{R_i^5}\left(\frac{35}{3}\cos^4\theta_i - 10\cos^2\theta_i + 1\right)$. $< r^n >_{3d}$ is the expectation value of the nth power, r^n, of the radial distance of a 3d orbital from the nucleus.

Through the Mn-O bond lengths and the expectation values of $< r^2 >_{3d}$ and $< r^4 >_{3d}$ for Mn^{3+} ions, it can easily be shown from Eqs.(6) and (7) that the contribution of the fourth-order CEF term of a distorted $Mn(Fe)O_6$ octahedron to the E_{JT} is so small, compared with that of the second-order CEF term, that we can neglect it. Thus Eq.(5) can be written as

$$E_{JT} \approx 4D_s = \frac{2e}{7}\sqrt{\frac{5}{\pi}}A_{20} < r^2 >_{3d}, \quad (8)$$

From Eqs.(1), (4) and (8), we can obtain an approximate relation between E_{JT} of Mn^{3+} ion and the quadrupole splitting for Fe^{3+} ion Δ (Fe^{3+})

$$E_{JT} = \frac{4\Delta(Fe^{3+})}{7Q\left(1+\frac{\eta^2}{3}\right)^{1/2}} < r^2 >_{3d}. \quad (9)$$

The quadrupole splitting for Mössbauer experiments is generally in units of mm/s. We may convert it to eV by a factor of E_γ/c, where E_γ=14.4keV for I= 3/2 $\leftrightarrow$1/2 transition of ^{57}Fe and c=3×10^{11}mm/s is the velocity of light. In the case of axial symmetry, η= 0. Using the approximate expectation value $< r^2 >$ of free Mn^{3+} ions, $< r^2 >$=0.003535nm^2 and Q=0.28×10^{-24}cm^2,[18−20] the Jahn–Teller coupling energy, E_{JT}, in the compounds is estimated and illustrated in Fig.3, and it is very close to the theoretical value.[21]

Figure 3 illustrates the quadrupole splitting corresponding to Fe^{3+} ions and Jahn–Teller coupling energy corresponding to Mn^{3+} ions in $Nd_{0.5}Pb_{0.5-x}Sr_xMn_{0.96}Fe_{0.04}O_3$ as a function of Sr concentration. With increasing Sr concentration, the quadrupole splitting and Jahn–Teller coupling decrease. Local structural distortion of $Mn(Fe)O_6$ octahedron in $Nd_{0.5}Pb_{1-x}Sr_xMn_{0.96}Fe_{0.04}O_3$ perovskites also decreases.

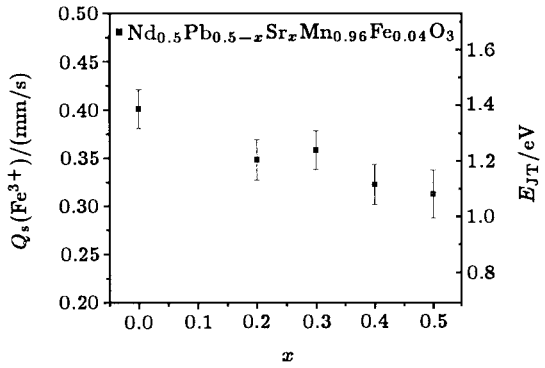


Fig.3. Curve shows the quadrupole splitting corresponding to Fe^{3+} ions and Jahn–Teller coupling energy corresponding to Mn^{3+} ions as a function of Sr concentration for the samples $Nd_{0.5}Pb_{0.5-x}Sr_xMn_{0.96}Fe_{0.04}O_3$ ($0.0 \leq x \leq 0.5$).

Figure 4 illustrates ρ–T curves of $Nd_{0.5}Pb_{0.5-x}Sr_x\ Mn_{0.96}\ Fe_{0.04}O_3$. The value of resistivity at room temperature drops with Sr doping. Clausen *et al*[22] regarded that the conductivity above T_c is due to hopping of localized magnetic polarons by magnetoresistance (MR) measurements at fields of up to 20T. It is related to the structural distortion. Substituting Sr for Pb decreases the Jahn–Teller distortion. At $T > T_c$, the disorder in the spins results in a decrease of DE coupling, but the Jahn–Teller coupling plays an important role in determining electrical resistance. A stronger Jahn–Teller coupling will localize the conduction electrons and make the hopping process difficult via DE coupling. When we substitute the equivalent quantity Fe for Mn, we fix the ratio of Mn^{3+} to Mn^{4+} also. Under the same DE condition, we think that the decrease of resistivity with increasing Sr concentration results more likely from the decrease of structure distortion of Jahn–Teller effect that can localize more conduction electrons than the DE above T_c.

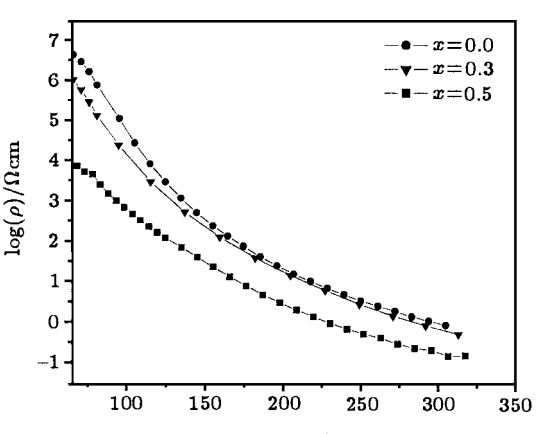


Fig.4. ρ-T curves of $Nd_{0.5}Pb_{0.5-x}Sr_xMn_{0.96}Fe_{0.04}O_3$ (x=0.0 (●), 0.3(▼), and 0.5 (■)) at room temperature and under 0T applied magnetic field.

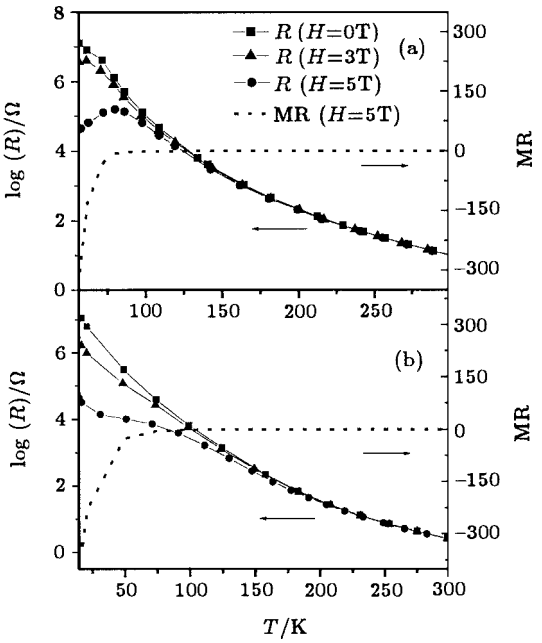


Fig.5. Temperature dependence of the resistance measured under 0T (■), 3T (▲) and 5T (●) applied magnetic fields and MR under 5T (dotted line) applied magnetic fields for sample $Nd_{0.5}Pb_{0.5-x}Sr_xMn_{0.96}Fe_{0.04}O_3$ with x=0.3 (a), x=0.5(b).

We also measured resistance in doped samples $Nd_{0.5}Pb_{0.5-x}Sr_xMn_{0.96}Fe_{0.04}O_3$ (x=0.0, 0.3, 0.5) under different magnetic fields. In the absence of applied field, samples are all insulator. MR behaviour does not occur in the sample with x=0.0. The magnetic field induces a metal–insulator transition for samples (x=0.3, 0.5). The temperature dependence of the resistance measured under 0T, 3T, and 5T applied fields and MR for samples (x=0.3, 0.5) are shown in Figs.5(a) and (b), respectively. The relative MR is defined as $[R(H) - R(0)]/R(H)$, and it reaches the maximum values of around 280, and 340 for x=0.3 and 0.5 samples respectively under a magnetic field of 5T. And the temperature of the maximum MR value decreases gradually with increasing x, because the conductivity above T_c can be ascribed to the hopping of localized magnetic polarons. A magnetic field can easily suppress spin fluctuations in the critical region. The resistance associated with magnetic disorder will be reduced in a magnetic field. In our previous paper,[13] we found that the quadrupole splitting of the Fe^{3+} has no obvious change with the change of temperature at $T > T_c$. So we think that the decrease of Jahn–Teller distortion delocalizes the conduction electrons and this can be regarded as another reason of the change of MR around the metal–insulator transition temperature.

4. Conclusion

We have studied XRD and Mössbauer spectra for system of $Nd_{0.5}Pb_{0.5-x}Sr_xMn_{0.96}Fe_{0.04}O_3$ ($0.0 \leq x \leq 0.5$) at room temperature. The results indicate the presence of local structural distortions. Through investigating transport properties of these compounds, we believe that these properties are related to the different ratios of Sr to Pb concentration, which can be attributed to the local structural distortion resulting from the Jahn–Teller effect of Mn^{3+} ions besides the DE coupling. Substituting Sr for Pb increases the symmetry of the crystal structure in samples $Nd_{0.5}Pb_{0.5-x}Sr_xMn_{0.96}Fe_{0.04}O_3$ and decreases the Jahn–Teller distortion. And for samples of x=0.3 and 0.5, MR increases and the temperature of the maximum MR value decreases with increasing x under a magnetic field of 5T. We think that this is also related to the delocalization of electrons resulting from the decrease of Jahn–Teller distortion.

Acknowledgement

Z. H. Cheng thanks the Alexander von Humboldt Foundation for financial support and generous donation of partial Mössbauer equipment.

References

[1] Jin S, Tiefel T, McMormack M, Fastnacht P A, Ramesh R and Chen L H 1994 *Science* **264** 413

[2] Lu Y *et al* 2003 *Chin. Phys.* **12** 1301

[3] Xiao C T *et al* 2003 *Acta Phys. Sin.* **52** 1245 (in Chinese)

[4] Millis A J, Littlewood P B and Shraiman B I 1995 *Phys. Rev. Lett.* **74** 5144

[5] Hwang H Y, Cheong S W, Radaelli P G, Marezio M and Batlogg B 1995 *Phys. Rev. Lett.* **75** 914

[6] Asamitsu A *et al* 1995 *Nature* (London) **373** 407

[7] Kawano H *et al* 1996 *Phys. Rev.* B **53** 2202

[8] Arulraj Anthony, Santhosh P N, Gopalan R Srinivasa, Guha Ayan, Raychaudhuri A K, Kumar N and Rao C N R 1998 *J. Phys: Condens. Matter* **10** 8497

[9] Rao C N R, Arulraj A, Santhosh P N and Cheetham A K 1998 *Chem. Mater.* **10** 2714

[10] Arulraj Anthony and Rao C N R 1999 *J. Solid State Chem.* **145** 557
[11] Clausen K N, Hayes W, Keen D A, Kusters R M, McGreevy R L and Singleton J 1989 *J. Phys: Condens. Matter* **1** 2721
[12] Radaelli P G *et al* 1997 *Phys. Rev.* B **56** 8265
[13] Cheng Z H *et al* 2003 *Appl. Phys. Lett.* **83** 1587
[14] Shannon R D 1976 *Acta Cryst.* A **32** 751
[15] Hunter B A and Howard C J 1998 *A computer program for Rietveld analysis of X-ray and Neutron powder diffraction patterns* (Lucas Heights Research Laboratories, NSW, Australia)
[16] Greewood N N and Gibb T C 1971 *Mössbauer spectroscopy* (London: Chapman and Hall)
[17] Griffith J S 1964 *The Theory of Transition-Metal Ion* (London: Cambridge University Press)
[18] Fraga S 1976 *Handbook of Atomic Data* (Amsterdam: Elsevier)
[19] Sharma R R and Das T P 1964 *J. Chem. Phys.* **41** 3581
[20] Artman J O, Muir A H, Jr. and Wiedersich H 1968 *Phys. Rev.* **173** 337
[21] Satpathy S, Popovic Z S and Vukajlovic F R 1996 *Phys. Rev. Lett.* **76** 960
[22] Clausen K N *et al* 1989 *J. Phys: Condens. Matter* **1** 2721